Spontaneous Scalarization of Neutron Stars in Scalar-Tensor Gravity

Eddie Revell

Department of Applied Mathematics and Theoretical Physics,
University of Cambridge

25^{th} April 2020

With thanks to my essay supervisor Dr Ulrich Sperhake, whose guidance has been most helpful.

Contents

1 Introduction

Einstein's theory of general relativity is one of the crowning achievements of human ingenuity and has so far passed all tests to very high precision. All such testing of the theory have taken place in the so called "weak field regime", where deviations from Newtonian gravity are noticeable but not extreme. Recent progress made in the field of gravitational wave interferometry has allowed physicists to probe even the strong field regime of the theory by investigating wave emissions from some of the most energetic events in the universe, including but not limited to black hole/neutron star mergers and stellar core collapse. This field therefore provides an ideal testing ground for general relativity in the high energy limit, and will thus either solidify our belief in its correctness, or point towards a new modification of the theory which differs from GR in this limit. Developing such a modification is a challenge because it must predict to high precision the same results as GR in all the weak field tests that have been passed to date, but provide significant measurable differences detectable by GW interferometers. The main idea of constructing such a theory is to modify Einstein's equations (or the corresponding Einstein-Hilbert action) by some "small" terms which only become significant in the high energy limit. One such theory which does this is *scalar-tensor gravity*, and while it is complicated enough to give such deviations, it remains sufficiently simple to provide predictions differing from GR that may be observable now. In particular, ST gravity predicts a phenomena known as *spontaneous scalarization* for sufficiently compact objects such as neutron stars, and the formation of such scalarized stars leads to the emission of gravitational waves unlike those predicted by GR. From a theoretical point of view, a modification to the theory in the high energy limit, such as that provided by ST gravity, is perfectly plausible because it is the same approach as is taken in quantum field theory which has seen considerable success in recent years.

This essay will first describe the theory of scalar-tensor gravity, laying out all necessary framework and equations. We will then derive spherically symmetric and static solutions in the theory, which provide the foundations for simulating stars and black holes, thus allowing scenarios such stellar core collapse to be numerically investigated. Then we will briefly discus the "post Newtonian formalism", a scheme that provides a description of how alternate theories of gravity may differ from Newton's, and how weak field experiments have provided stringent constraints on the allowable alternate theories. Finally, we move on to describing the process of spontaneous scalarization of neutron stars, and gravitational wave emission produced in their collapse. In particular, we will see that ST gravity predicts dipole GW radiation (as opposed to quadrupole radiation, as predicted by GR) and thus how the detection of such a signal could constitute *smoking gun evidence* for our new theory.

2 Scalar-Tensor Gravity

A general theory in $d+1$ dimensional spacetime in which gravity is coupled with multiple scalar fields can be described by the action:

$$S = \frac{1}{16\pi}\int d^{d+1}x\ \sqrt{-g}\big(F(\phi)R - \gamma_{ab}(\phi)g^{\mu\nu}\partial_\mu\phi^a\partial_\nu\phi^b - U(\phi)\big) + S_M[\mathbf{\Phi}, g_{\mu\nu}] \tag{2.1}$$

Where, as usual we have a metric $g_{\mu\nu}$, a matter field $\mathbf{\Phi}$ and matter interaction S_M. F and U are (arbitrary) functions of the N scalar fields ϕ^a $(a = 1, ..., N)$, with the scalar fields living on a manifold with metric γ_{ab}. It is easy to see that we recover Einstein's theory of gravity in the case $F(\phi) = 1,\ \gamma = 0,\ U = 0$. This generalisation of GR is reasonable because it is similar to the modern approach to particle physics, which is to include higher order terms to a Lagrangian from a non-interacting theory in order to capture the non-trivial interactions between various fields. It is also very similar to the Nambu-Goto action from string theory, a field that has seen mixed success in recent years.

In this essay, we will study the theory with $N = 1$, $F(\phi) = \phi$ and $\gamma_{11}(\phi) = \frac{\omega(\phi)}{\phi}$ for some function ω. This is known as the *Bergmann-Wigoner formulation*:

$$\boxed{S = \frac{1}{16\pi}\int d^{d+1}x\ \sqrt{-g}\left(\phi R - \frac{\omega(\phi)}{\phi}g^{\mu\nu}\partial_\mu\phi\partial_\nu\phi - U(\phi)\right) + S_M[\mathbf{\Phi}, g_{\mu\nu}]} \tag{2.2}$$

We will keep d general for now, but will later restrict ourselves to the case $d = 3$.

2.1 Which Frame?

The action (2.2) is referred to as the *Jordan-frame* action. It is advantageous in that the metric $g_{\mu\nu}$ (and hence Ricci scalar) and the matter interaction are physical, and so predict the properties of geodesics and suchlike in our observable universe. However, the treatment of this action is mathematically difficult due to both the presence of the function ω in the coupling term between the scalar field and the metric, and also because ϕ is coupled to the Ricci scalar.

The mathematical treatment of the theory is made significantly easier by means of conformally transforming the metric. In particular, we may redefine ϕ via $\varphi = \varphi(\phi)$ (so $U(\phi) \to V(\varphi)$) and transform our metric by $g_{\mu\nu} \to g^*_{\mu\nu} = A^{-2}(\varphi) g_{\mu\nu}$ so that the action (2.2) becomes the *Einstein-frame* action:

$$\boxed{S = \frac{1}{16\pi} \int d^{d+1}x \, \sqrt{-g^*}\big(R^* - 2g^{*\mu\nu}\partial_\mu\varphi\partial_\nu\varphi - V(\varphi)\big) + S_M[\mathbf{\Phi}, A^2(\varphi)g^*_{\mu\nu}]} \tag{2.3}$$

The case $V(\varphi) = 0$ will be referred to as *massless* scalar-tensor gravity, while $V(\varphi) = \frac{1}{2}\mu^2\varphi^2$ as *massive* scalar-tensor gravity[1] (with mass μ). We also have the freedom to add interaction terms such as $\lambda\varphi^4$ to V, which will be discussed later.

Claim 2.1. The above conformal transformation really does work, with the Jordan-frame and Einstein-frame quantities being related by:

$$\phi = A^{1-d}(\varphi) \tag{2.4}$$

$$d + (d-1)\omega(\phi) = \frac{2}{d-1}\alpha(\varphi)^{-2} \tag{2.5}$$

Where $\alpha(\varphi) = d(\ln\ A(\varphi))/d\varphi$

Remark: We began by saying the theory is determined by the choice of $\omega(\phi)$ and scalar potential. However, we see that from the above we can get $d + (d-1)\omega(A^{-2}(\varphi)) = 2/(d-1)\alpha(\varphi)^{-2}$, and hence knowing ω determines A via this differential equation, which subsequently determines α. Conversely, knowing α determines A, which determines ω. *Hence we may equivalently describe our theory by a choice of α and scalar potential in the Einstein-frame.*

Proof. Under the conformal transformation $g_{\mu\nu} \to g^*_{\mu\nu} = A^{-2}(\varphi)g_{\mu\nu}$, the Ricci scalar transforms as $R \to R^*$, with:

$$R^* = A^2(\varphi)\left(R - \frac{4d}{d-1}A(\varphi)^{\frac{d-1}{2}}\nabla^\mu\nabla_\mu\big(A(\varphi)^{\frac{1-d}{2}}\big)\right) \tag{2.6}$$

The proof of this being omitted (it is a long exercise in following through the definitions). More easily, $g = \det(g_{\mu\nu}) = \det(A^2(\varphi)g^*_{\mu\nu}) = A^{2(d+1)}g^*$, and hence:

$$\sqrt{-g} = A^{d+1}(\varphi)\sqrt{-g^*} \tag{2.7}$$

We may use the above to see that the action (2.2) becomes:

$$S = \frac{1}{16\pi}\int d^{d+1}x\, \sqrt{-g^*}A^{d+1}(\varphi)\left[\phi A^{-2}(\varphi)R^* + \frac{4d}{d-1}\phi A^{\frac{d-1}{2}}(\varphi)\nabla^\mu\nabla_\mu A^{\frac{1-d}{2}}(\varphi) - \frac{\omega(\phi)}{\phi}g^{\mu\nu}\partial_\mu\phi\partial_\nu\phi - U(\phi)\right] + S_M[\mathbf{\Phi}, A^2(\varphi)g^*_{\mu\nu}]$$

Now, we could just substitute in the claimed result and see that it works, but this is not particularly instructive. Instead, we will derive these results.

[1] One might wonder why this is an appropriate potential to describe a massive scalar field. Indeed, the Einstein-frame is in some sense unphysical, and so if anything we should really be introducing $U(\phi) = \frac{1}{2}\mu'^2\phi^2$ for a physical mass μ' in the Jordan-frame, and seeing what sort of potential V this transforms to when we change frame. This matter is still subject to much debate within the field, and generally it is considered best to work with the Einstein-frame. We shall discus this issue no further in this essay.

The key idea of the Einstein-frame is to decouple the scalar field ϕ from the Ricci scalar R. Thus, considering the first term, we require $A^{d+1}(\varphi) \times \phi \times A^{-2}(\varphi) = 1$, and hence the result (2.4). The action then becomes:

$$S = \frac{1}{16\pi}\int d^{d+1}x\ \sqrt{-g^*}\Big[R^* - \omega(\phi)A^{2d-2}(\varphi)g^{*\mu\nu}\partial_\mu A^{1-d}(\varphi)\partial_\nu A^{1-d}(\varphi) - A^{d+1}(\varphi)U(\phi)\Big] + \frac{1}{16\pi}\int d^{d+1}x\ \sqrt{-g}\Big[\frac{4d}{d-1}A^{\frac{1-d}{2}}(\varphi)\nabla^\mu\nabla_\mu A^{\frac{1-d}{2}}(\varphi)\Big] + S_M[\mathbf{\Phi}, A^2(\varphi)g^*_{\mu\nu}]$$

Observe that we have written the term with the second derivative separately, and transformed $\sqrt{-g^*}$ back to $\sqrt{-g}$ in this term. This is because the covariant derivative ∇^μ assumes that the Levi-Civita connections are those associated with the metric $g_{\mu\nu}$, not $g^*_{\mu\nu}$, and hence to use the divergence theorem we must have a volume element $\sqrt{-g}$, not $\sqrt{-g^*}$. Using the divergence theorem and writing $V(\varphi) = A^{d+1}(\varphi)U(\phi(\varphi))$, we find after collecting all the terms that:

$$\begin{aligned}S &= \frac{1}{16\pi}\int d^{d+1}x\ \sqrt{-g^*}\Big[R^* - g^{*\mu\nu}A^{d-1}\Big(\omega(\phi)A^{d-1}(\varphi)\partial_\mu A^{1-d}(\varphi)\partial_\nu A^{1-d}(\varphi) + \frac{4d}{1-d}\partial_\mu A^{\frac{1-d}{2}}(\varphi)\partial_\nu A^{\frac{1-d}{2}}(\varphi)\Big) \\ &\qquad - V(\varphi)\Big] + S_M[\mathbf{\Phi}, A^2(\varphi)g^*_{\mu\nu}] \\ &= \frac{1}{16\pi}\int d^{d+1}x\ \sqrt{-g^*}\Big[R^* + (1-d)(d-(1-d)\omega(\varphi))A^{-2}(\varphi)\Big(\frac{dA}{d\varphi}\Big)^2 g^{*\mu\nu}\partial_\mu\varphi\partial_\nu\varphi - V(\varphi)\Big] \\ &\qquad + S_M[\mathbf{\Phi}, A^2(\varphi)g^*_{\mu\nu}]\end{aligned}$$

Where in going from the first line to the second we used the chain rule. Thus, to get the action (2.3), we require $A^{-2}(\varphi)(dA/d\varphi)^2(1-d)(d-(1-d)\omega(\phi)) = -2$, from which the result (2.5) follows. □

2.2 Equations of Motion

The principle of least action allows us to determine the dynamics of our metric and scalar field in each of the Jordan and Einstein frames. The phenomenon of spontaneous scalarization to be studied is best treated from the latter of these frames, and so here we will present a brief outline of how the equations of motion for $g^*_{\mu\nu}$ and φ are derived, with the results in the Jordan frame being omitted.

Claim 2.2. The equations of motion for $g^*_{\mu\nu}$ and φ are given by:

$$R^*_{\mu\nu} = 2\nabla^*_\mu\varphi\nabla^*_\nu\varphi + 8\pi\big(T^*_{\mu\nu} - \frac{1}{d-1}T^*g^*_{\mu\nu}\big) + g^*_{\mu\nu}\frac{1}{d-1}V(\varphi) \tag{2.8}$$

$$\Box^*\varphi = -4\pi\alpha(\varphi)T^* + \frac{1}{4}\frac{dV}{d\varphi} \tag{2.9}$$

Where $T^*_{\mu\nu} = 2(-g^*)^{-1/2}\delta S_M/\delta g^*_{\mu\nu}$.

Remark: These are slightly different to those listed in [2] in that the potential V is non zero and the number of spacetime dimensions is $d+1$, rather than $3+1$.

Proof. We begin by varying φ. Under the infinitesimal transformation $\varphi \to \varphi + \delta\varphi$, we have:

$$\begin{aligned}\delta S &= \frac{1}{16\pi}\int d^{d+1}x\ \delta\varphi\sqrt{-g^*}\Big(4\Box^*\varphi - \frac{dV}{d\varphi}\Big) + S_M[\mathbf{\Phi}, A^2(\varphi+\delta\varphi)g^*_{\mu\nu}] - S_M[\mathbf{\Phi}, A^2(\varphi)g^*_{\mu\nu}] \\ &= \frac{1}{16\pi}\int d^{d+1}x\ \delta\varphi\sqrt{-g^*}\Big(4\Box^*\varphi - \frac{dV}{d\varphi}\Big) + S_M[\mathbf{\Phi}, A^2(\varphi)(g^*_{\mu\nu} + 2\alpha(\varphi)g^*_{\mu\nu}\delta\varphi)] - S_M[\mathbf{\Phi}, A^2(\varphi)g^*_{\mu\nu}] \\ &\implies \frac{1}{16\pi}\Big(4\Box^*\varphi - \frac{dV}{d\varphi}\Big) + 2\alpha(\varphi)g^{*\mu\nu}\frac{\delta S_M(\mathbf{\Phi}, A^2(\varphi)g^*_{\mu\nu})}{\delta g^*_{\mu\nu}} = 0 \\ &\implies \Box^*\varphi = -4\pi\alpha(\varphi)T^* + \frac{1}{4}\frac{dV}{d\varphi}\end{aligned}$$

Which is the result (2.9). Next we vary $g^*_{\mu\nu} \to g^*_{\mu\nu} + \delta g^*_{\mu\nu}$. Famously, the variation of $\int d^{d+1}x\ \sqrt{-g^*}R^*$ gives a contribution $-G^{*\mu\nu}\sqrt{-g^*}$ to the equation of motion while the variation of the volume element is $\delta\sqrt{-g^*} = 1/2\sqrt{-g^*}g^{*\mu\nu}\delta g^*_{\mu\nu}$ (see e.g. [5]). This is enough information to compute the equation of motion:

$$
\begin{aligned}
&-G^{*\mu\nu} + 2\nabla^{*\mu}\varphi\nabla^{*\nu}\varphi - g^{*\mu\nu}\nabla^*_\sigma\varphi\nabla^{*\sigma}\varphi - \frac{1}{2}g^{*\mu\nu}V(\varphi) + 8\pi T^{*\mu\nu} = 0 \\
\implies &G^*_{\mu\nu} - 2\nabla^*_\mu\varphi\nabla^*_\nu\varphi + g^*_{\mu\nu}\nabla^*_\sigma\varphi\nabla^{*\sigma}\varphi + \frac{1}{2}g^*_{\mu\nu}V(\varphi) - 8\pi T^*_{\mu\nu} = 0 \qquad (*) \\
\implies &R^* - \frac{1}{2}(d+1)R^* + (d-1)\nabla^*_\sigma\varphi\nabla^{*\sigma}\varphi + \frac{1}{2}(d+1)V(\varphi) - 8\pi T^* = 0 \quad \text{(take the trace)} \\
\implies &\frac{-1}{2}R^* + \nabla^*_\sigma\varphi\nabla^{*\sigma}\varphi + \frac{d+1}{2(d-1)}V(\varphi) - \frac{8\pi}{d-1}T^* = 0 \\
\implies &R^*_{\mu\nu} = 2\nabla^*_\mu\varphi\nabla^*_\nu\varphi + 8\pi\big(T^*_{\mu\nu} - \frac{1}{d-1}T^*g^*_{\mu\nu}\big) + g^*_{\mu\nu}\frac{1}{d-1}V(\varphi)
\end{aligned}
$$

Where to get the last line we substitute the result from line four into the second line. This is (2.8). □

3 Static Spherical Solutions in GR and Scalar-Tensor Gravity

We will now restrict our attention to $d = 3$, to study the $3+1$ spacetime we live in.

Because General Relativity is a special case of scalar-tensor gravity, we may derive static spherical solutions to the equations of the former by first deriving those for scalar-tensor gravity and then appropriately setting α, φ and V. The most general physical metric $g_{\mu\nu}$ that is spherically symmetric and static may be written in the form:

$$ds^2 = g_{\mu\nu}dx^\mu dx^\nu = e^{2\Phi(r)}dt^2 + e^{2\Psi(r)}dr^2 + r^2(d\theta^2 + \sin^2\theta d\phi^2) \tag{3.1}$$

An important question to further our study of scalar-tensor theories is to ask what symmetries, if any, are inherited by the new metric $g^*_{\mu\nu} = A^{-2}(\varphi)g_{\mu\nu}$. Fortunately it is easy to see[2] that for a spherically symmetric scalar field with no time dependence, $\varphi = \varphi(r)$, if our physical metric $g_{\mu\nu}$ is spherically symmetric and static, so is $g^*_{\mu\nu}$.

Thus, we will now assume the convention of [2] and write our general spherically symmetric, static metric as:

$$ds^{*2} = g^*_{\mu\nu}dx^\mu dx^\nu = -e^{\nu(r)}dt^2 + \frac{dr^2}{1-2\mu(r)/r} + r^2(d\theta^2 + \sin^2\theta d\phi^2) \tag{3.2}$$

Which we may compare to (3.1) by identifying $2\Phi(r) = \nu(r)$ and $2\Psi(r) = \ln(1/(1-2\mu/r))$.

3.1 The Generalised Tolman-Oppenheimer-Volkoff Equations

Our goal is to solve for $\mu(r)$, $\nu(r)$, $\varphi(r)$ and $P(r)$, given an equation of state $\rho = \rho(P)$ and energy momentum tensor $T^{\mu\nu}$, by using the equations (2.8) and (2.9) and the stress-energy balance condition $\nabla_\mu T^{\mu\nu} = 0$. To begin, for a metric with line element 3.2, the tt and rr components of the Einstein Tensor are given by:

$$G^{*tt} = \frac{2e^{-\nu(r)}}{r^2}\mu'(r) \qquad G^{*rr} = \frac{1}{r^2}\left(1 - \frac{2\mu(r)}{r}\right)^2\left[r\nu'(r) - \frac{2\mu(r)}{r-2\mu(r)}\right] \tag{3.3}$$

(see e.g. [16].) find a better reference - perhaps a book. Now we will assume that our matter distribution takes a perfect fluid form, so that the energy momentum tensor is given by:

$$T^{\mu\nu} = (\epsilon + P)u^\mu u^\nu + Pg^{\mu\nu} \qquad \text{with } u^\mu u_\mu = -1 \tag{3.4}$$

[2] If you don't believe me, write $ds^{*2} = g^*_{\mu\nu}dx^\mu dx^\nu = A^{-2}(\varphi)ds^2$, with ds^2 as is given in (3.1). Then use the change of variables $\tilde{r} = r/A(\varphi)$, $e^{\tilde{\Phi}} = e^\Phi/A(\varphi)$ and $e^{\tilde{\Psi}} = A(\varphi)e^\Psi/(1 - rA'(\varphi))$, with ' denoting d/dr, to see that the line element can be written in the form (3.1).

For energy density ϵ and pressure P, both of which are functions of spacetime. Under the static and spherically symmetric assumptions, we have ϵ and P depending only on r, and also that $u = u(r) \propto (1,0,0,0)$ (in (t,r,θ,ϕ) coordinates). Then:

$$u^\mu u_\mu = -1 \iff A^{-2}(\varphi) g^{*\mu\nu} u_\mu u_\nu = -1 \implies u_t = A(\varphi) e^{\frac{1}{2}\nu(r)}$$

(Up to a choice of plus/minus sign). Hence $u^t = -A^{-1}(\varphi) e^{\frac{-1}{2}\nu(r)}$, and:

$$T^{\mu\nu} = A^{-2}(\varphi)\mathrm{diag}\left\{\epsilon(r)e^{-\nu(r)}, P(r)\left(1-\frac{2\mu(r)}{r}\right), \frac{P(r)}{r^2}, \frac{P(r)}{r^2\sin^2\theta}\right\} \tag{3.5}$$

The final ingredient we need is to relate $T^{\mu\nu}$ to $T^{*\mu\nu}$:

$$T^{\mu\nu} = 2(-g)^{-1/2}\frac{\delta S_M(\mathbf{\Phi}, g_{\mu\nu})}{\delta g_{\mu\nu}} = 2A^{-4}(\varphi)(-g^*)^{-1/2}\frac{\delta S_M(\mathbf{\Phi}, A^2(\varphi)g^*_{\mu\nu})}{\delta g^*_{\sigma\rho}}\frac{\delta g^*_{\sigma\rho}}{\delta g_{\mu\nu}} = A^{-6}(\varphi)T^{*\mu\nu} \tag{3.6}$$

Rather than use the equation (2.8) as in [2], it is in this author's opinion that it is in fact easier to use the intermediate equation in the proof of claim 2.2 labelled by $(*)$, which itself may be rewritten as:

$$G^{*\mu\nu} = 2\nabla^{*\mu}\varphi\nabla^{*\nu}\varphi - g^{*\mu\nu}\nabla^*_\sigma\varphi\nabla^{*\sigma}\varphi - \frac{1}{2}g^{*\mu\nu}V(\varphi) + 8\pi T^{*\mu\nu} \tag{3.7}$$

Combining (3.5) and (3.6) and substituting into the above, we have:

$$\begin{aligned} tt \text{ component:} \quad & \mu'(r) = 4\pi A^4(\varphi) r^2\epsilon + \frac{1}{2}r(r-2\mu)\varphi'^2 + \frac{r^2}{4}V(\varphi) \\ rr \text{ component:} \quad & \nu'(r) = \frac{8\pi r^2 A^4(\varphi)P}{r-2\mu} + r\varphi'^2 + \frac{2\mu}{r(r-2\mu)} - \frac{r^2}{2(r-2\mu)}V(\varphi) \end{aligned}$$

Meanwhile, the equation (2.9) for φ tells us:

$$\begin{aligned} & g^{*\mu\nu}(\partial_\mu\partial_\nu\varphi - \Gamma^{*\alpha}_{\mu\nu}\partial_\alpha\varphi) = -4\pi\alpha(\varphi)A^4(\varphi)(-\epsilon+3P) + \frac{1}{4}\frac{dV}{d\varphi} \\ \implies & g^{*rr}\varphi'' - g^{*\mu\nu}\Gamma^{*r}_{\mu\nu}\varphi' = -4\pi\alpha(\varphi)A^4(\varphi)(-\epsilon+3P) + \frac{1}{4}\frac{dV}{d\varphi} \end{aligned}$$

Relevant Christoffel symbols may be found in the appendix. Some of them depend on $\mu'(r)$ and $\nu'(r)$, but we already know these by the previous results and, after some algebra, we get:

$$\varphi'' = \frac{4\pi r A^4(\varphi)}{r-2\mu}\big(\alpha(\varphi)(\epsilon-3P) + r(\epsilon-P)\varphi'\big) - \frac{2(r-\mu)}{r(r-2\mu)}\varphi' + \frac{r^2\varphi'}{2(r-2\mu)}V(\varphi) + \frac{r}{4(r-2\mu)}\frac{dV}{d\varphi}$$

The final equation can be found by considering the $\theta\theta$ (or $\phi\phi$) component of (3.7), or alternatively by using the r component of the stress-energy balance equation. It turns out the latter is easier:

$$\nabla_\mu T^{\mu r} = 0 \iff \partial_r T^{rr} + \Gamma^\mu_{\mu r}T^{rr} + \Gamma^r_{\mu\nu}T^{\mu\nu} = 0$$

We want to use the Christoffel symbols for the metric $g^*_{\mu\nu}$ listed in the appendix. Working directly from the definition of the Christoffel symbols, it is not hard to see that these are related to the Christoffel symbols for the metric $g_{\mu\nu}$ by $\Gamma^\mu_{\nu\rho} = \Gamma^{*\mu}_{\nu\rho} + \alpha(\varphi)(\delta^\mu_\rho\partial_\nu\varphi + \delta^\mu_\nu\partial_\rho\varphi - g^{*\mu\alpha}g^*_{\rho\nu}\partial_\alpha\varphi)$. Using this relation in the above and working through the algebra, we arrive at:

$$P'(r) = -(P+\epsilon)\left(\frac{1}{2}\nu'(r) + \varphi'\alpha(\varphi)\right) = -(P+\epsilon)\left(\frac{4\pi r^2 A^4(\varphi)P}{r-2\mu} + \frac{1}{2}r\phi'^2 + \frac{\mu}{r(r-2\mu)} - \frac{r^2}{4(r-2\mu)}V(\varphi) + \alpha(\varphi)\varphi'\right)$$

We have now derived four equations for five variables, $\mu(r)$, $\nu(r)$, $\varphi(r)$, $P(r)$, and $\epsilon(r)$. Thermodynamics gives us an equation of state relating P and ϵ, and so in fact there are only four unknowns and in principle we may solve this system.

To summarise, we have the *generalised Tolman-Oppenheimer-Volkoff quations*:

$$\mu'(r) = 4\pi A^4(\varphi) r^2 \epsilon + \frac{1}{2} r(r-2\mu)\varphi'^2 + \frac{r^2}{4} V(\varphi) \tag{3.8}$$

$$\nu'(r) = \frac{8\pi r^2 A^4(\varphi) P}{r-2\mu} + r\varphi'^2 + \frac{2\mu}{r(r-2\mu)} - \frac{r^2}{2(r-2\mu)} V(\varphi) \tag{3.9}$$

$$\varphi'' = \frac{4\pi r A^4(\varphi)}{r-2\mu}\big(\alpha(\varphi)(\epsilon - 3P) + r(\epsilon - P)\varphi'\big) - \frac{2(r-\mu)}{r(r-2\mu)}\varphi' + \frac{r^2\varphi'}{2(r-2\mu)} V(\varphi) + \frac{r}{4(r-2\mu)} \frac{dV}{d\varphi} \tag{3.10}$$

$$P'(r) = -(P+\epsilon)\left(\frac{4\pi r^2 A^4(\varphi) P}{r-2\mu} + \frac{1}{2} r\varphi'^2 + \frac{\mu}{r(r-2\mu)} - \frac{r^2}{4(r-2\mu)} V(\varphi) + \alpha(\varphi)\varphi'\right) \tag{3.11}$$

To be solved with some equation of state $P = P(\epsilon)$.

3.2 Stars in GR

3.2.1 Inside the Star

By setting $A = 1$, $V = 0$ and $\varphi = \text{const.}$ in the system of equations (3.8), (3.9), (3.11) (and ignoring the equation (3.10) for the dynamics of φ) we recover the usual TOV equations used in the study of static, spherical spacetimes. We will also use the replacement $\mu \leftrightarrow m$ to identify μ with mass as is common in the literature. The first of these equations gives:

$$m(r) = 4\pi \int_0^r \epsilon(r) r^2 dr + m_* \tag{3.12}$$

With m_* being the mass $m(0)$. However, since the manifold is smooth at $r = 0$ a point on S^2 a small radius r must be a distance r from $r = 0$, and so:

$$r \approx \int_0^r \left(1 - \frac{m(r')}{r'}\right)^{-\frac{1}{2}} dr' \implies 1 - \frac{2m(r)}{r}\bigg|_{r=0} = 1 \iff \frac{m(r)}{r}\bigg|_{r=0} = 0 \tag{3.13}$$

Therefore, since $m(r)$ is smooth, it is at least $\mathcal{O}(r^2)$ as $r \to 0$ and hence $m_* = 0$.

Now that we know $m(r)$, we may in principle integrate our expression (3.11) to find P so long as we are given an equation of state relating P and ϵ and an initial value of P at $r = 0$, P_c say. In particular, we will stop this integration when the pressure reaches[3] 0 since this defines the surface of the star. The value of r the integration stopped at, R, is thus the radius of the star ($R = R(P_c)$). We may then use (3.13) to determine the function $m(r)$, and hence the total mass of the star $M = m(R)$ is a function of P_c as well, $M = M(P_c)$. Finally, we may find $\nu(r)$ by integrating (3.9) inwards from the surface of the star, subject to the matching condition $\nu(R) = \log(1 - 2M/R)$ (see (3.14) in next section).

Observe that once we have found the point $P = 0$ by numerical integration, we automatically determine $R = R(P_c)$, $M = M(P_c)$ and $\epsilon_c = \epsilon(P_c)$ (from the equation of state). Hence solutions to stars in GR are described by a *one parameter family of solutions*, indexed by P_c. We may invert these to let R index the family of solutions, and write P_c, ϵ_c and M as functions of R.

3.2.2 Outside the Star

Birkhoff's theorem tells us that outside the star we need only consider the Schwarzschild metric, and so everything outside is determined uniquely by the ADM mass of the star. Given the radius of the star, R, we

[3]With the physically reasonable assumptions $P, \epsilon > 0$ and $r > 2\mu(r)$ (i.e. no singularities), (3.11) tells us that P is a positive decreasing function and so the physical intuition of pressure vanishing on the surface is mathematically feasible when we perform numerical integration.

choose $\nu(R)$ so that our metric is continuous at the surface. We find that:

$$\nu(R) = \log\left(1 - \frac{2M}{R}\right) \qquad M := m(R) \tag{3.14}$$

3.3 Stars in Scalar-Tensor Gravity

We will first study the generalised TOV equations for general V and coupling function $A(\varphi)$. As in the GR case, it is not possible to solve these equations explicitly, and a similar argument is used to show the existence of a two-parameter family of solutions.

As before, our manifold must be smooth at $r = 0$. Therefore, by considering (3.9), we see that $\mu/[r(r-2\mu)]$ must be finite as $r \to 0$, from which we deduce[4] $\mu(r) = \mathcal{O}(r^2)$ as $r \to 0$. By further differentiating (3.8), we may in fact deduce $\mu(r) = \mathcal{O}(r^3)$ as $r \to 0$. This is important because we then see in (3.9) that $\nu'(0) = 0$. Because only $\nu'(r)$ appears in the generalised TOV equations, we may WLOG set $\nu(0) = 0$. We will denote the values of φ and P at $r = 0$ by φ_c and P_c respectively. Finally, because of spherical symmetry, P must be stationary at $r = 0$ and hence $P'(0) = 0$, which implies in (3.11) $\varphi'(0) = 0$.

We may thus start with the initial conditions $\mu(0) = \mu'(0) = \nu(0) = \nu'(0) = 0$, $P(0) = P_c$, $P'(0) = 0$, $\varphi(0) = \varphi_c$, $\varphi'(0) = 0$ and integrate the generalised TOV equations until the point $P = 0$, which defines the surface of our star. While it is intuitively reasonable that initial conditions should lead to a well defined surface with $P = 0$, it is not mathematically obvious that our numerical integration will succeed in reaching $P = 0$, indeed (3.11) needn't be strictly negative given certain choices of $V(\varphi)$ and $\alpha(\varphi)$. The subtlety here is that we expect the cosmological values of φ to be vanishingly small, and hence the last four terms in (3.11) become negligible for large enough r (and the coupling function approaches unity), which reduces to the GR case where integration was successful. Therefore, reaching $P = 0$ is a consequence of the boundary conditions we impose on the system at infinity, rather than being due to the structure of the generalised TOV equations themselves.

At the surface of the star, we match our interior solution to the spherically symmetric, static external one. Unfortunately, the exterior in the full Scalar-Tensor theory case is considerably more complicated than the Schwarzchild metric, and cannot be expressed in a closed form in the (t, r, θ, ϕ) coordinates we have used so far. We will simplify matters by now restricting to the massless case (V=0) and changing coordinates.

3.3.1 Just Coordinates

Rather than use the usual Schwarzchild coordinates, we introduce *Just coordinates* [2, 4], under which the line element takes the form:

$$ds^{*2} = -e^{\rho(\tilde{r})}d\tilde{t}^2 + e^{-\rho(\tilde{r})}(d\tilde{r}^2 + e^{\lambda(\tilde{r})}(d\theta^2 + \sin^2\theta d\phi^2) \tag{3.15}$$

We set $T^* = 0$ (vacuum $\iff T = 0 \iff T^* = 0$ by (3.6)) and $V = 0$ (by assumption) in (2.8) and (2.9). These may be treated in a similar fashion to how we derived the generalised TOV equations in section (3.1), but are now solvable in full generality. We find that:

$$\rho(\tilde{r}) = \ln\left(1 - \frac{a}{\tilde{r}}\right)^{\frac{b}{a}} \tag{3.16}$$

$$\lambda(\tilde{r}) = \ln\left(\tilde{r}^2 - a\tilde{r}\right) \tag{3.17}$$

$$\varphi(\tilde{r}) = \varphi_0 + \frac{d}{a}\ln\left(1 - \frac{a}{\tilde{r}}\right) \tag{3.18}$$

Where a, b and d are constants of integration satisfying $a^2 - b^2 = 4d^2$. Physically relevant quantities are the total ADM mass of g^*, M, and the "total scalar charge" ω defined via $\varphi = \varphi_0 + \omega/r + \mathcal{O}(1/r^2)$ as $r \to \infty$.

[4] We could alternatively come to this conclusion by using the same trick as in (3.13) and using (3.8) to find $\mu'(0) = 0$ also.

By Taylor expanding our solution $\varphi(\tilde{r})$ and making the identification $\tilde{r} \sim r$ for large r, we see that $d = -\omega$. It can also be shown $b = 2M$ [4].

By comparing the Schwarzschild form of the line element (3.2) to that of Just (3.15), we have the relations:

$$r = \tilde{r}\left(1 - \frac{a}{\tilde{r}}\right)^{\frac{a-b}{2a}} \tag{3.19}$$

$$1 - \frac{2\mu}{r} = \left(1 - \frac{a}{\tilde{r}}\right)^{-1}\left(1 - \frac{a+b}{2\tilde{r}}\right)^{2} \tag{3.20}$$

$$\nu(r) = \frac{b}{a}\log\left(1 - \frac{a}{\tilde{r}}\right) \tag{3.21}$$

Where we have also used the results (3.16) - (3.18).

3.3.2 Matching the Interior and Exterior Solutions

The general solution obtained in Just coordinates in the previous section allows us to match the interior solution to the exterior one and in particular allows us to write φ_0, ω and M in terms of quantities at the surface of the star, which we will distinguish by writing a subscript s.

Begin by comparing (3.17) and (3.21) to see that $\varphi = \varphi_0 + d\nu/b$. Differentiating with respect to r and setting $r = r_s$, we see that $d/b = \varphi_s'/\nu_s'$. Recalling $d = -\omega$ and $b = 2M$, we therefore have:

$$-\frac{\omega}{M} = \frac{2\varphi_s'}{\nu_s'}$$

Next, we may eliminate $\tilde{r}$ from (3.20) by use of (3.21) to get:

$$1 - \frac{2\mu_s}{r_s} = \frac{1}{a^2}\left[a\cosh\left(\frac{a\nu_s}{2b}\right) + b\sinh\left(\frac{a\nu_s}{2b}\right)\right]^2 \tag{$*$}$$

Next we recall the restriction $a^2 - b^2 = 4d^2$ and observe that we may use the change of variables $\cosh\alpha = a/2d$, $\sinh\alpha = b/2d$, which allows us to use the addition formula for hyperbolic functions in the above. We get:

$$\begin{aligned}
1 - \frac{2\mu_s}{r_s} &= \frac{4d^2}{a^2}\cosh^2\left(\alpha + \frac{a\nu_s}{2b}\right) \\
\iff \tanh\left(\alpha + \frac{a\nu_s}{2b}\right) &= \sqrt{1 - \frac{4d^2}{a^2}\left(1 - \frac{2\mu_s}{r^s}\right)^{-1}} \\
\iff \tanh\left(\alpha + \frac{a\nu_s}{2b}\right) &= \frac{\nu_s' - 2r_s\varphi_s'^2}{\sqrt{\nu_s'^2 + 4\varphi_s'^2}}
\end{aligned}$$

Where in the last line we used (3.9) to replace μ_s in favour of ν_s' and φ_s'. Finally, making use of the formula $\operatorname{arctanh}\theta - \operatorname{arctanh}\phi = (\theta - \phi)/(1 - \theta\phi)$ and again making use of $a^2 - b^2 = 4d^2$ and $d/b = \varphi_s'/\nu_s'$, we arrive at:

$$\nu_s = -\frac{2\nu_s'}{\sqrt{\nu_s'^2 + 4\varphi_s'^2}}\operatorname{arctanh}\left(\frac{\sqrt{\nu_s'^2 + 4\varphi_s'^2}}{\nu_s' + 2/r_s}\right) \tag{3.22}$$

Another useful equation can be obtained by using (3.21) to eliminate $\tilde{r}$ from (3.19), which gives:

$$r_s = \frac{1}{2}ae^{-\nu_s/2}\operatorname{cosech}\left(\frac{a\nu_s}{2b}\right) \tag{3.23}$$

Putting everything together[5], we arrive at the relations in [2]:

$$\frac{-\omega}{M} = \frac{2\varphi_s'}{\nu_s'} \tag{3.24}$$

$$\varphi_0 = \varphi_s + \frac{2\varphi_s'}{\sqrt{\nu_s'^2 + 4\varphi_s'^2}} \operatorname{arctanh}\left(\frac{\sqrt{\nu_s'^2 + 4\varphi_s'^2}}{\nu_s' + 2/r_s} \right) \tag{3.25}$$

$$M = \frac{r_s^2 \nu_s'}{2}\left(1 - \frac{2\mu_s}{r_s}\right)^{\frac{1}{2}} \exp\left[- \frac{\nu_s'}{\sqrt{\nu_s'^2 + 4\varphi_s'^2}} \operatorname{arctanh}\left(\frac{\sqrt{\nu_s'^2 + 4\varphi_s'^2}}{\nu_s' + 2/r_s} \right)\right] \tag{3.26}$$

We have thus outlined the general method for relating the symmetric static solution outside of the star to quantities on its surface, which may be found by integrating the generalised TOV equations from $r = 0$ with the initial conditions $\mu(0) = \mu'(0) = \nu(0) = \nu'(0) = 0$, $P(0) = P_c$, $P'(0) = 0$, $\varphi(0) = \varphi_c$, $\varphi'(0) = 0$.

4 The PPN Formalism

The theory of General Relativity has so far passed all tests with high precision. Nevertheless, it is possible that small deviations from the theory may be inevitable - there are several theories describing a possible mechanism for these deviations, scalar-tensor gravity being one of them. This rich theoretical framework needs to be matched with a rigorous and precise method of experiment in order to test predictions and restrict possible parameter spaces. The necessity for such a scheme lead to the development of the *Parametrized Post Newtonian (PPN) formalism.*

4.1 A Brief Outline of the PPN Formalism

Before the success of gravitational wave interferometers, tests of GR could only be done by observations of the motion of celestial bodies, be it in our solar system or those elsewhere in the universe. Such experiments probe the structure of the metric tensor, which we may write as:

$$\begin{aligned} g_{00} &= -1 + 2\left(\frac{M}{r}\right) - 2\tilde{\beta}\left(\frac{M}{r}\right)^2 + \mathcal{O}\left(\frac{M}{r}\right)^3 \\ g_{0j} &= \mathcal{O}\left(\frac{M}{r}\right) \\ g_{jk} &= (1 + 2\tilde{\gamma}M/r)\delta_{jk} + \mathcal{O}\left(\frac{M}{r}\right)^2 \end{aligned} \tag{4.1}$$

Where we have expanded in powers of the Newtonian potential M/r, with higher order terms being increasingly negligible in the weak field regime (M being the mass of our Sun, since it is in our solar system where experiments take place). $\tilde{\beta}$ and $\tilde{\gamma}$ are *post Newtonian parameters* - we may expand further to give a set of 10 such parameters describing g_{00} to order four, g_{0j} to order three and g_{ij} to order two, but these are not necessary[6] for our discussion of scalar-tensor gravity. More detail may be found in [18].

General relativity predicts $\tilde{\beta} = \tilde{\gamma} = 1$, while one finds that in the massless Bergmann-Wigoner scalar-tensor theory [1]:

$$\tilde{\gamma} = \frac{1 + \omega(\phi_0)}{2 + \omega(\phi_0)} \qquad \text{and} \qquad \tilde{\beta} = 1 + \frac{\omega'(\phi_0)}{(3 + 2\omega(\phi_0))^2(4 + 2\omega(\phi_0))} \tag{4.2}$$

[5]We obtained the second equation by substituting (3.22) into $\varphi_s = \varphi_0 + d\nu_s/b$, and the third by multiplying (3.23) by the square-root of equation $(*)$ and then again using (3.22).

[6]In both classical general relativity and scalar-tensor gravity, the remaining eight post Newtonian parameters are all zero. Also, often in the literature there is no "tilde" above β, γ - we have included them here to distinguish from other functions, such as $\beta = \partial\alpha/\partial\varphi$.

Where we assume that ϕ takes an asymptotic value ϕ_0, and $\omega'(\phi_0) = d\omega/d\phi|_{\phi_0}$. We may equivalently write these with quantities in the Einstein frame as:

$$\tilde{\gamma} = \frac{1-\alpha_0^2}{1+\alpha_0^2} \qquad \text{and} \qquad \tilde{\beta} = 1 + \frac{1}{2}\frac{\alpha_0^2\beta_0}{(1+\alpha_0^2)^2} \tag{4.3}$$

Where $\alpha_0 = \alpha(\varphi_0)$ and $\beta_0 = \partial\alpha/\partial\varphi|_{\varphi_0}$.

4.2 Experimental Constraints on Massless Scalar-Tensor Gravity

Several experiments have been done in the weak field limit to provide constraints on α_0 and β_0, the first being the results of the Cassini space mission and the second being the results of binary pulsar experiments. We will briefly describe them here, and the bounds on configuration space for α_0 and β_0 may be found in Figure 1.

Cassini Space Spacecraft: The Cassini-Huygens space probe was sent to study Saturn and its system in 1997. Because of its large distance from earth, a *Doppler* method could be used to determine changes in frequency when pinging signals from Earth, to the spacecraft, and back again. Indeed, the fractional frequency shift $\gamma_{\text{gr}} = \Delta\nu/\nu$ for such a signal is [6, 18]:

$$\gamma_{\text{gr}} = -2(1+\tilde{\gamma})\frac{GM_\odot}{c^3 b}\frac{\mathrm{d}b}{\mathrm{d}t} \tag{4.4}$$

With b being the impact parameter, $M_\odot \sim 2\times 10^{30}$ the solar mass, G and c the usual gravitational constant and speed of light respectively. Because of the large distance of the probe from Earth, $\mathrm{d}b/\mathrm{d}t$ is approximately the orbital velocity of the earth, about 30 km s^{-1}. During the experiment, the impact parameter was ~ 1 au, and $\gamma_{\text{gr}} \sim 10^{-10}$ was measured. Plugging these into the above gives an order of magnitude estimate $|\tilde{\gamma}-1| \lesssim 10^{-5}$. Taking into account possible sources of error as in [6], the actual result is:

$$\tilde{\gamma} = 1 + (2.1 \pm 2.3)\times 10^{-5} \tag{4.5}$$

The reason such a Doppler shift experiment had not been done on spacecraft before Cassini is because there was too much noise in signals being pinged to get a good bound - Cassini used novel communication methods making the removal of such noise possible. In 2017, the mission was ended by deliberately crashing Cassini into Saturn, to ensure no possible biological contamination of Saturn's moons.

Binary Pulsar Experiments: Many alternate theories of gravity, scalar-tensor gravity being one of them, predict the emission of dipole gravitational wave radiation in addition to the usual quadrupole emission that GR predicts. One way to observe such radiation would be to use a GW interferometer and measure it directly. However, we can also deduce bounds on GW waves emitted by looking at how a binary star systems orbits decay. In order for this method to be viable, it is necessary one of the stars in the system is a *pulsar*, a rapidly rotating highly magnetised neutron star which emits electromagnetic radiation from its magnetic poles. Thus, every time one of the poles faces Earth, we get a periodic flash of EM radiation allowing very accurate time keeping, and hence measurements, of the system we are studying. Measured results from such a system can then be used to constrain theory space of scalar-tensor gravity. The results of this are displayed in Figure 1, where the systems PSR J0348+0432 [8] and PSR J1738+033 [10] were studied.

Remark: As we will see, the far field solution for massless scalar tensor gravity decays like $1/r$, whereas in the massive theory it decays as $e^{-m_\varphi r}/r$. Because of the difference in these solutions, the binary pulsar methods used to constrain β in the massless case are nowhere near as effective, and as a result the allowed region for β is much larger than that presented in Figure 1 for the massive theory.

5 Spontaneous Scalarization

Scalar-Tensor gravity gives all the same predictions in the weak field, slowly moving regime as general relativity does, but somewhat remarkably gives significant macroscopic differences away from this regime.

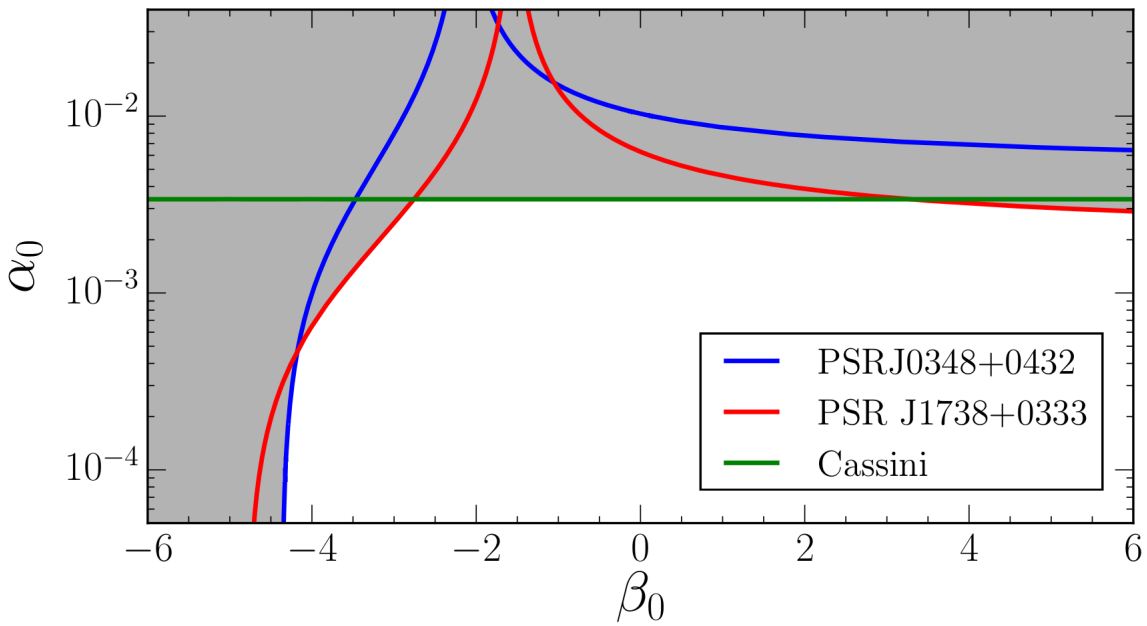

Figure 1: The allowed region for α_0 and β_0 in parameter space, taken from [14]. The blue and red lines are from two binary pulsar experiments discussed, while the green line is from the Cassini space mission. Note that General Relativity lies at $\alpha_0 = \beta_0 = 0$.

Our first port of call in investigating the extreme physics predicted by both theories might be to investigate black holes. However, due to strong restrictions placed on these objects by the so called *no-hair theorems* [3, 13], this is not the best place to look. The most promising object to investigate therefore is the next most extreme, the neutron star, which is not subject to any of the aforementioned no-hair theorem constraints. Indeed, we will see that scalar-tensor gravity predicts macroscopically different properties for neutron stars, and can lead to the phenomena of *spontaneous scalarization*, something which is not predicted by GR.

5.1 A Heuristic Argument for Scalarization

The governing equations (2.8) and (2.9) are non-linear and complicated to analyse, even in a static spacetime with spherical symmetry the resulting generalised TOV equations (3.8 - 3.11) are in general not easily solved in a closed analytic form for a given equation of state $\epsilon = \epsilon(P)$. In this section we will show heuristically that for a wide range of theory space a phenomena known as *scalarization* can take place in certain circumstances.

Consider the theory with $A(\varphi) = \exp(\beta\varphi^2/2)$, so that $\alpha(\varphi) = \beta\varphi$ and $\beta(\varphi) = \beta = \text{const.}$ in a spherically symmetric spacetime containing a single star (centred at the origin) of radius R, mass M and self-gravity $s = M/R$. Further, we approximate $\Box^*\varphi \approx (-\partial_t^2 + \nabla^2)\varphi$ and $T^* = A^4(\varphi)(3P - \epsilon) \approx -\epsilon \approx -\rho$, the (constant) density of the star. Additionally, we will assume the potential V is given by only a mass term, $V(\varphi) = 2m_\varphi^2\varphi^2$. The equation for the dynamics of φ, (2.9) reduces to:

$$-\frac{\partial^2\varphi}{\partial t^2} + \frac{1}{r^2}\frac{\partial}{\partial r}\left(r^2\frac{\partial\varphi}{\partial r}\right) = \begin{cases}(4\pi\beta\rho + m_\varphi^2)\varphi & r < R\\ m_\varphi^2\varphi & r > R\end{cases} \tag{5.1}$$

Where we made use of spherically symmetry to use only the radial part of the Laplacian. By use of the ansatz $\varphi(t, r) = r^p f(t, r)$, and observing that $p = -1$ reduces the problem to a forced wave equation, we have:

$$-\partial_t^2 f + \partial_r^2 f = \begin{cases}\sigma\kappa^2 f & r < R\\ m_\varphi^2 f & r > R\end{cases} \qquad \kappa = \sqrt{|4\pi\beta\rho + m_\varphi^2|} \quad , \quad \sigma = \text{sign}(4\pi\beta\rho + m_\varphi^2) \tag{5.2}$$

5.1.1 Static Solutions

We will analyse (5.2) in the static case, which physically represents the solution after dynamical processes have ceased and equilibrium has been reached. We will write the solutions inside and outside the star as φ_{int} and φ_{ext} respectively. There are two cases to consider:

1. **Massless case:** For $m_\varphi = 0$, it is easy to see that outside the star we have $\varphi_{\text{ext}} = \varphi_0 + \omega/r$. Insisting that the solution at $r = 0$ is non-singular, the interior is given by:

$$\varphi_{\text{int}}(r) = \begin{cases} \frac{\varphi_c}{\kappa r}\sin(\kappa r) & \text{if } \beta < 0 \\ \frac{\varphi_c}{\kappa r}\sinh(\kappa r) & \text{if } \beta > 0 \end{cases} \tag{5.3}$$

   Finally, we must match conditions at the boundary $r = R$. Denoting quantities on the boundary $r \gtrless R$ by $\pm$ respectively, continuity implies $\varphi^- = \varphi^+$ while integrating over the boundary gives the matching condition $[\varphi']^+_- = -2(\varphi^+ - \varphi^-)/R = 0$. This gives us:

$$\underbrace{\frac{\varphi_c}{\kappa R}\text{sin(h)}(\kappa R) = \varphi_0 + \frac{\omega}{R}}_{\text{(from continuity)}} \qquad \text{and} \qquad \underbrace{\varphi_c = \frac{\varphi_0}{\cos(\text{h})(\kappa R)}}_{\text{(from derivative)}} \tag{5.4}$$

   Where we use sin/cos if $\beta < 0$ and sinh/cosh if $\beta > 0$.

2. **Massive case:** The interior is similar to the massless case:

$$\varphi_{\text{int}}(r) = \begin{cases} \frac{\varphi_c}{\kappa r}\sin(\kappa r) & \text{if } \sigma = -1 \\ \frac{\varphi_c}{\kappa r}\sinh(\kappa r) & \text{if } \sigma = 1 \end{cases} \tag{5.5}$$

   Insisting that the field φ remains finite as $r \to \infty$, the only possible solution is $\varphi_{\text{ext}} = \omega\exp(-m_\varphi r)/r$ for a constant ω that is still consistent with our definition of scalar charge ($\varphi = \varphi_0 + \omega/r$ as $r \to \infty$). The same matching conditions as before give us:

$$\underbrace{\omega = \frac{\varphi_c}{\kappa}e^{m_\varphi R}\text{sin(h)}(\kappa R)}_{\text{(from continuity)}} \qquad \text{and} \qquad \underbrace{\tan(\text{h})(\kappa R) = \frac{-\kappa}{m_\varphi}}_{\text{(from derivative)}} \tag{5.6}$$

   Where we use sin/cos if $\sigma = -1$ and sinh/cosh if $\sigma = 1$.

In both cases we can observe the phenomena of *scalarization* - the solution for φ takes non-trivial values within the star despite having a vanishing cosmological value ($\varphi = 0$ at infinity). This is most easily seen in the massless case: If $\beta < 0$, the second equation in (5.4) implies $\varphi_c > \varphi_0$. Even in the limit $\varphi_0 \to 0$ this non trivial result can hold, by taking $\kappa R \to -\pi/2$. The condition $\kappa R = -\pi/2$ is equivalent to $M/R = \pi^2/(12|\beta|)$. For neutron stars, $M/R \gtrsim 0.2$, so we expect scalarization if $\beta \lesssim -4$. On the other-hand, if $\beta > 0$, $\varphi_c < \varphi_0$ and so deviations from GR are damped in this case.

For the massive case, consider the second equation of (5.6). Observe that for $\sigma = 1$ there are no positive solutions to this equation. On the other-hand, when $\sigma = -1$ we have $\tan(\kappa R) = -\kappa/m_\varphi$. This equation is complicated in the sense that it relates ρ, β, m_φ and R. If we write $\rho = 3s/(4\pi R^2)$, s being the self-gravity of the star, we have:

$$\tan(x) = -kx \qquad \text{where} \quad k = \frac{1}{Rm_\varphi} \quad \text{and} \quad x = \kappa R = \sqrt{|3s\beta + k^{-2}|} \tag{5.7}$$

We therefore see that we have reduced the equation to a form where it effectively only depends on two variables, x and k, making analysis easier. The solutions to this equation (for fixed k) are plotted in Figure 2. Observe that in the limit $m_\varphi \to 0$ with R remaining finite, we have $k \to \infty$ so that $x \to \pi/2$, recovering the $m_\varphi = 0$ result $M/R = \pi^2/(12|\beta|)$. We also observe that decreasing k makes the solution move away from $x = \pi/2$ in the positive direction, and hence the value of $s|\beta|$ must increase and so the region of β for

which scalarization can occur is decreased from the $\beta \lesssim -4$ we obtained in the massless case. To make this more concrete, let us assume $s \gtrsim s_0$ for neutron stars, which gives the inequality $\beta \lesssim \beta_0$ for the star to be scalarized when we plug into the equation $s = \pi^2/(12|\beta|)$ (previously, $s_0 = 0.2$ and $\beta_0 = -4$). Now assume R is finite and m_φ is small so that $k = 1/\epsilon$ for some small ϵ. Then to leading order we find that $x = \pi/2 + 2\epsilon/\pi$ and hence $s|\beta| = (\pi^2/4 + 2\epsilon)/3$. For neutron stars with $s \gtrsim s_0$ this gives us $\beta = \beta_0 - 2\epsilon/(3s_0)$, and so our inequality is only changed by a small first order amount. *Therefore, provided that m_φ is small, this does not significantly effect the bound on β.*

The fact that a massive term does not significantly effect the bound on β is crucial to keeping our theory alive. We saw previously that in the massless theory β_0 was severely constrained by the results of binary pulsar observations (see Figure 1) to approximately the edge of the allowed region $\beta \lesssim -4$. However, the presence of a mass term means this bound is no longer applicable and the allowed region of β is much larger, making scalarization much more probable in the massive theory [15].

Remark: Finding scalarized solutions in this simplified model boiled down to solving an equation with a countable infinity of solutions (Figure 2). However, at least in the massless[7] case, these form a sequence of disconnected energetically less favourable equilibrium configurations and therefore are not associated with any physical ambiguities [2].

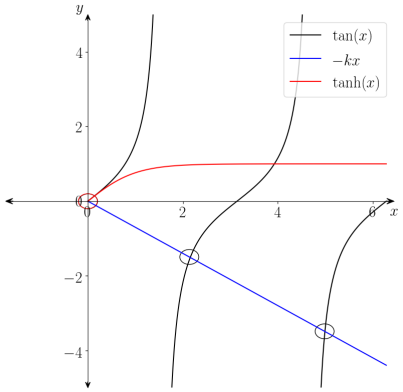

Figure 2: Graphical solutions to the second equation in (5.7). As can be seen in the case $\sigma = -1$, there are infinitely many solutions, but for the case $\sigma = 1$ the only solution lies at the origin.

5.1.2 Dynamics and Spontaneity

So far we have established, at least heuristically, that scalarized stars are possible. This section serves to explain why this process is described as *spontaneous*. We will first consider the case that φ is dependent on time in (5.2) to show an extremely fast attainment of equilibrium. We assume now that $\sigma = -1$, since we have already ruled out scalarization in the $\sigma = 1$ case.

Begin by taking the Fourier transform of (5.2) with respect to the r variable. We deduce that the solution outside the star is then:

$$\varphi_{\text{ext}}(t, r) = \frac{1}{2\pi r} \int_{-\infty}^{\infty} e^{ikr} A(k) \sin\left(t\sqrt{k^2 + m_\varphi^2} + \omega_0(k)\right) \, dk \tag{5.8}$$

For functions $A(k)$ and $\omega_0(k)$ which needn't be determined. The import observation is that for fixed r, there is no exponential dependence on t. On the other-hand, for the interior of the star we have:

$$\varphi_{\text{int}}(t, r) = \frac{1}{2\pi r} \int_{-\infty}^{\infty} e^{ikr} A'(k) \sin\left(t\sqrt{k^2 - \kappa^2} + \omega_0'(k)\right) \, dk \tag{5.9}$$

For functions $A'(k)$ and $\omega_0'(k)$ which again needn't be determined. The crucial part here is that, for fixed r, we have exponential blow up in the region $|k| < |\kappa|$ (because the argument in sine becomes complex). This is known as a *Tachyon instability*. Such an instability would be bad for our theory, but we realise that it is just a consequence of the simplifying assumption of removing the $A^4(\varphi)$ term in the initial equation - the inclusion of this term would be to stop the growth at larger t. The condition $|k| < |\kappa|$ may be rewritten as

[7] I am unable to find any studies mentioning this in the massive case, but suspect it is still true.

$\lambda > \lambda_{\text{eff}}/\sqrt{1-(\lambda_{\text{eff}}/\lambda_\varphi)^2}$, where we have defined $\lambda = 2\pi/k$ and:

$$\lambda_\varphi = 2\pi/m_\varphi \qquad \text{(The } \textit{Compton wavelength}\text{)} \tag{5.10}$$

$$\lambda_{\text{eff}} = \sqrt{\frac{\pi}{\rho|\beta|}} \tag{5.11}$$

For our Tachyon instability to exist, we also require that half of such a wavelength fits inside the star, $\lambda/2 < 2R \implies \lambda_{\text{eff}} \lesssim 4R$. This can be rearranged to give $s \gtrsim \pi^2/(12|\beta|)$ as we saw before, giving the bound $\beta \lesssim -4$ for the scalarization of neutron stars.

Therefore, due to the existence of these wave-modes that grow exponentially fast (at least initially), we deduce that the scalarization of the star is a very rapid process, and hence it is referred to as *spontaneous*. Indeed, a characteristic time for a star to become scalarized is given by $\lambda_\varphi/(2\pi) = \hbar/(c^2 m_\varphi)$ (restoring units of c and $\hbar$.) The constraint $10^{-16}\text{eV} < m_\varphi < 10^{-9}\text{eV}$ [15] then gives an estimate of a time to scalarize ranging between 10^{-6} seconds and 1 second, which is very fast indeed.

5.2 Numerical Simulations

So far we have only shown heuristically that we might expect non-trivial scalar-field dynamics for certain values of β. However, it isn't obvious whether these are physical or merely a consequence of the simplifying assumptions we made in the previous section (namely that $\Box^* = -\partial_t^2 + \nabla^2$, $A(\varphi) \approx 1$ and $T = -\rho =$ constant inside the star). To show that spontaneous scalarization can occur when solving the full non-linear equations we must solve them numerically to high accuracy using a computer. Fortunately, several studies have been done on them, and the purpose of this section is to discus briefly their key findings.

5.2.1 Initial Conditions and Equations of State

In order to solve the generalised TOV equations for a static star, or for more general dynamics involving time such as stellar collapse, it is necessary to implement initial conditions and decide upon an appropriate equation of state for our matter. In the studies discussed here, the latter is assumed to be *polytropic*, meaning that P and ρ are related by an equation of the form:

$$P = K\rho^\Gamma \tag{5.12}$$

Where K is a constant of proportionality and Γ is a *adiabatic index*. The values of K and Γ are chosen to best fit equations of states of stars deduced from theoretical principles and observations, it is a whole field of study in its own right and the details are not discussed here. This equation of state may be generalised to consist of piecewise polytropic states, an important example being different polytropic indices above and below the nuclear density $\rho_{\text{nuc}} \approx 2 \times 10^{14}\text{g/cm}^3$:

$$P = \begin{cases} K_1\rho^{\Gamma_1} & \text{if } \rho < \rho_{\text{nuc}} \\ K_2\rho^{\Gamma_2} & \text{if } \rho \geq \rho_{\text{nuc}} \end{cases} \tag{5.13}$$

Because the star is an isolated system, we can use the first law of thermodynamics as applied to an adiabatic precess to then determine the specific internal energy, which is used in the numerical scheme in involving the generalised TOV equations (3.8-3.11). We can make the model even better by combining such states to make a *hybrid* EOS, typically of the form $P = P_{\text{c}} + P_{\text{th}}$, where the *cold* part P_{c} is of the form (5.13) while the *thermal* part is given by $P_{\text{th}} = (\Gamma_{\text{th}} - 1)\rho\epsilon_{\text{th}}$, where ϵ_{th} is the internal energy due to the thermal part, which may be determined from the primitive variable ϵ used in the numerical scheme. The EOS is therefore characterised by the three adiabatic indices Γ_1, Γ_2 and Γ_{th}.

The remaining ingredient we require for computational methods is an initial state of our star. A simple profile which qualitatively captures the behaviour is a polytrope of the form (5.12) with $K = 4.935 \times 10^{14}$, $\Gamma = 4/3$ and constant central mass density $\rho_c = 10^{10}\text{g cm}^{-3}$ [14]. On the other-hand, we may use more realistic *Woosley-Heger* (WH) profiles [7], which model zero-age-main-sequence stars. In the literature, stars of 12 and 40 solar masses respectively are studied, which we will refer to as WH12 and WH40.

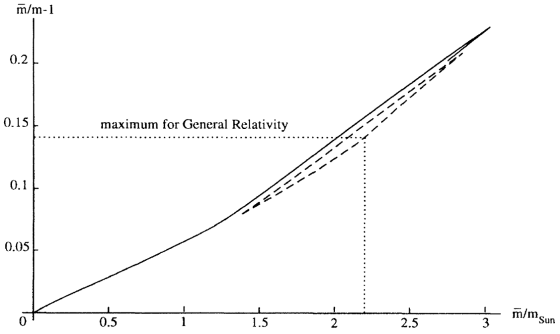

(a) Fractional binding energy vs baryonic mass.

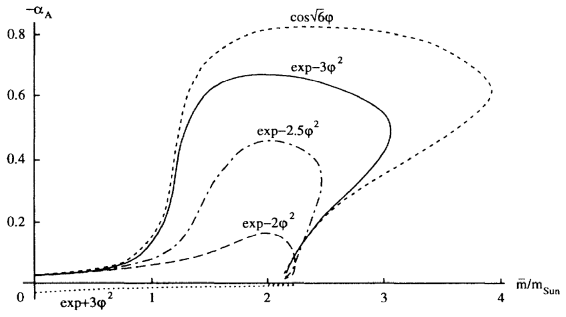

(b) Scalar coupling constant vs baryonic mass

Figure 3: Results of T. Damour and G. Esposito-Farèse's 1993 work [2]. (a) illustrates how the fractional binding energy of a star in scalar-tensor gravity changes with baryonic mass, in the theory where $A(\varphi) = \exp(-3\varphi^2)$ and $\varphi_0 = 0.0043$ using a polytrope with $\Gamma = 2.34$ and $K = 0.0195$. The most energetically favourable equilibrium configuration is represented by the solid black line, while the dashed lines represent a sequence of (less energetically favourable) equilibrium configurations. Because they are disconnected from the solid black line, they are considered unphysical. The dotted black lines indicate the turning point for the maximum in GR. (b) shows how the "scalar coupling constant" $-\omega/M$ varies with baryonic mass for various different coupling functions for the same star as in (a). This coupling constant effectively describes the "strength" of the interaction between our scalar field and the star, and the extent to which it can scalarize.

5.2.2 Discussion of Results

Now that we have discussed appropriate physical conditions for stars, we are ready to numerically investigate the consequences of our theory once we specify a coupling function $A(\varphi)$ (or $\alpha(\varphi)$) and scalar potential. The results of some studies are presented here:

Nonperturbative Strong-Field Effects in Tensor-Scalar Theories of Gravitation [2]
A polytropic equation of state of the form (5.12) is used in the massless theory ($V = 0$) for coupling functions of the form $A(\varphi) = \exp(k\varphi^2)$ for $k \in \mathbb{R}$, and the system of equations solved are the generalised TOV equations (3.8 - 3.10). As we mentioned in section 5.1.1, the fractional binding energy is increased for stars in scalar-tensor gravity, compared to their GR counterparts, and there is a sequence of disconnected equilibrium configurations (each less energetically favourable than the other). The effective scalar coupling constant is found to be sensitive to the choice of k but largely insensitive to variations in φ_0 the cosmological value of φ (see section 5.1.1 for discussions of this result).

Long-Lived Inverse Chirp Signals Frome Core Collapse in Massive Scalar-Tensor Gravity [14]
In this study, spherically symmetric core collapse is investigated. The equations for numerical simulation are similar to the generalised TOV equations but include extra terms reflecting the fact that the scenario is no longer static. The three initial density profiles (polytropic, WH12 and WH40) and hybrid EOS (with $\Gamma_1 = 1.3$, $\Gamma_2 = 2.5$ and $\Gamma_{\text{th}} = 1.35$) discussed in the previous section are used, while the coupling function[8] is given by $A(\varphi) = \exp[\alpha_0\varphi + \beta_0\varphi^2/2]$ with $\varphi_0 = 0$. In the study, it was found that core collapse can indeed lead to scalarized neutron stars, and for the WH40 model a scalarized black hole was formed. These findings are important because they demonstrate that scalarization can occur in a dynamical scenario and is not just a consequence of the time independent assumptions made in Damour and Esposito-Farèse's work.

[8](This is equivalent to $A(\varphi) = \exp[\beta_0\varphi^2]$ with non-zero φ_0)

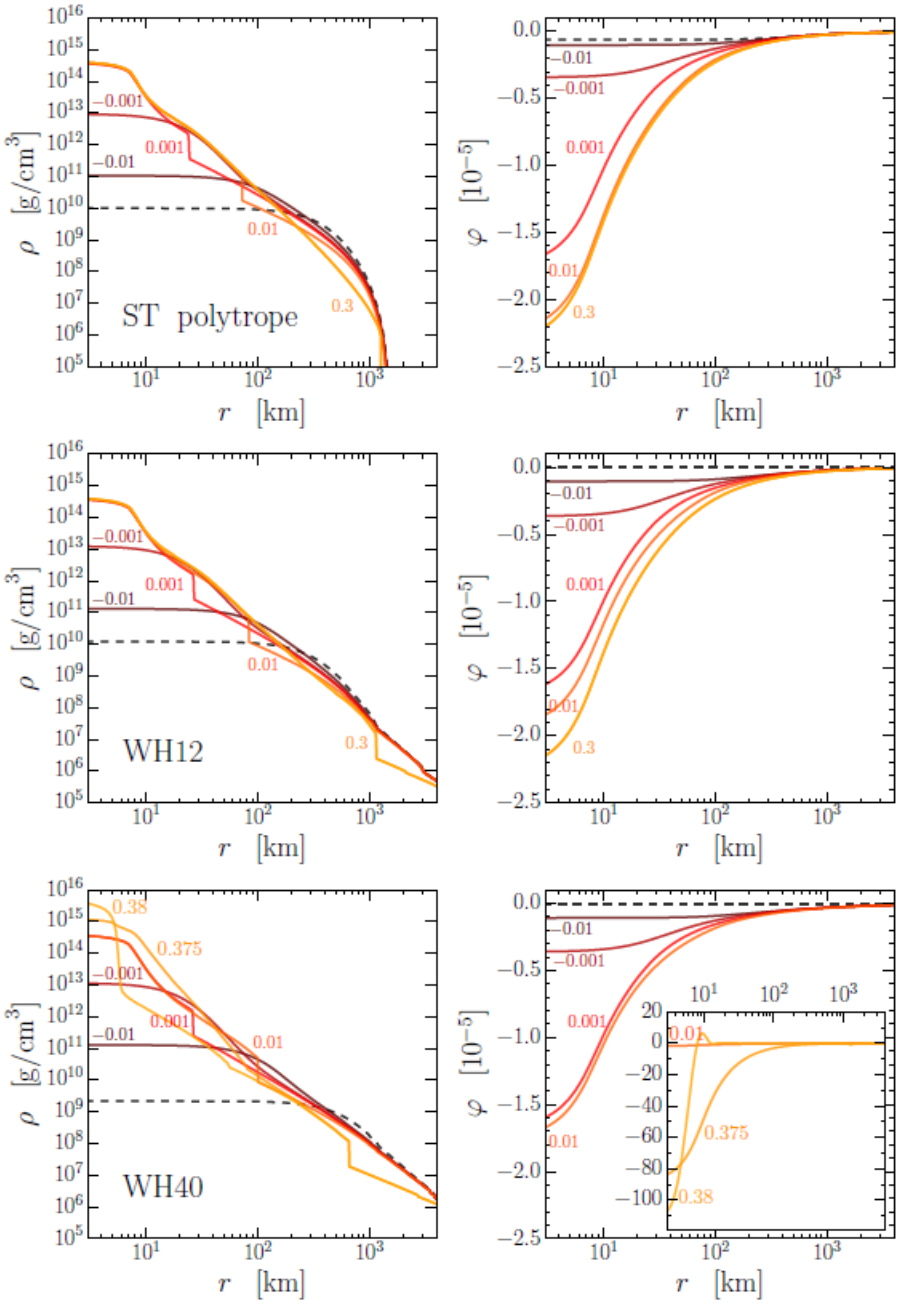

Figure 4: The results of the core collapse simulations performed in [14]. The top, middle and bottom rows correspond to the polytrope, WH12 and WH40 initial profiles respectively, and a hybrid equation of state is used (see section 5.2.1). The simulations were run with $\beta_0 = -4.35$ which sits on the boundary allowed by Figure 1 and is sufficiently negative for scalarization to occur. The evolution of mass density ρ and the scalar field φ are shown in the left and right columns respectively, at timesteps $t - t_b = -0.01, -0.001, 0.001, 0.1, 0.3, 0.3, 0.375$ seconds (t_b being the time for core-bounce to occur). Observe the steepening of the initial density profiles in the left hand figures, demonstrating the formation of compact objects after core bounce, while the right hand figures show us in all cases that this object is scalarized. In fact, the ST polytrope and WH12 initial profiles form scalarized neutron stars, while the most massive WH40 profile forms a scalarized black hole.

6 Gravitational Waves in GR and Scalar-Tensor Gravity

6.1 Scalar Waves

We will begin by discussing the far field solution for φ in the case of a massive potential $V(\varphi) = 2m_\varphi^2\varphi^2$. With the assumption that far from any matter source the spacetime is almost Minkowski, the equation (2.9) reduces to exactly that of (5.1) in the $r > R$ regime. We will analyse this by again identifying that $f = r\varphi$ satisfies the forced wave equation $-\partial_t^2 f + \partial_r^2 f = m_\varphi^2 f$ as we did in (5.2). This time we will Fourier transform with respect to the t coordinate to find:

$$\tilde{f}(\omega, r) = \tilde{f}(\omega, r_{\text{ex}}) \begin{cases} \exp\big(-i\sqrt{\omega^2 - \omega_\varphi^2}(r - r_{\text{ex}})\big) & \text{for } \omega < -\omega_\varphi \\ \exp\big(+i\sqrt{\omega^2 - \omega_\varphi^2}(r - r_{\text{ex}})\big) & \text{for } \omega > -\omega_\varphi \end{cases} \tag{6.1}$$

Where we have defined the *Compton frequency*[9] $\omega_\varphi = m_\varphi$. Notice that when $|\omega| < |\omega_\varphi|$, f dies of exponentially. This means there is a sharp frequency cut-off in frequency-domain power spectrum of the signal, which can be seen in Figure 5. r_{ex} is the *extraction radius* for when we perform numerical simulations, and may be thought of here as a boundary condition.

Remark: Let assume for simplicity that f is even in t. This is justifiable because we are only interested in the physics with $t \geq 0$ and so may freely extend f to an even function in $t \leq 0$. Now, because f is even we see that $\tilde{f}(-\omega, r) = \frac{1}{2\pi}\int_{-\infty}^{\infty} f(t)\exp(i\omega t)\, dt = \frac{1}{2\pi}\int_{-\infty}^{\infty} f(-t)\exp(-i\omega t)\, dt = \tilde{f}(\omega, r)$ where in the first equality we used the change of variables $t \to -t$ and in the second we used the fact f is even. Hence $\tilde{f}$ *is also even, in the* ω *argument.* We will see why this is useful in the next section.

6.1.1 The Method of Stationary Phase

For the purposes of this essay, the *stationary phase approximation* (SPA) is a method for determining the large time behaviour of a function of the form $\Psi(x,t) = \int_{-\infty}^{\infty} A(k)\exp(ikx - i\omega(k)t)$.

Let us briefly present an intuitive picture of the result, by considering an analogy to plane waves being generated by a source at $x = 0$. For an observer at large t, x, one would expect only waves with velocity $V = x/t$ to reach us, so we can substitute this to get $\Phi(x,t) = \int_{-\infty}^{\infty} A(k)\exp(it\psi(k))$ with $\psi(k) = kV - \omega(k)$. It can be shown that in the regions where ψ is monotonic (so $\psi'(k) \neq 0$) this integral decays exponentially fast [12], but at points where $\psi'(k) = 0$ we get significant contribution to the integral (physically, this corresponds to less cancellation due to changes in phase in these regions, which contributes most to the integral). Then, in the case of only one stationary point α of ψ, a Taylor series expansion yields the far field solution:

$$\Phi = \left(\frac{2\pi}{|\psi''(\alpha)|t}\right)^{\frac{1}{2}} A(\alpha)e^{i\psi(\alpha)t + i\frac{\pi}{4}\text{sign}(\psi''(\alpha))} \tag{6.2}$$

If there is more than one stationary point α, we just add up the contributions from each. If $\psi''(\alpha) = 0$, we continue the aforementioned Taylor expansion to the first non zero $\psi^n(\alpha)$, but this detail will not be relevant to us.

Physical interpretation of group velocity: Solving the equation $\Omega'(k) = V$ physically corresponds to finding the unique wave number whose group velocity propagates at speed V. Therefore the method of stationary phase physically means that if we, the observer, are located at a far distance x from the initial disturbance, then at time t, we only see contributions from the wave packet that travels at speed $V = x/t$, because all other wave packets travel at a different speed and thus have already passed us/not reached us yet.

[9] This is in units $\hbar = 1$, and so while the definition is trivial here it is different when we reintroduce units - namely $\omega_\varphi = m_\varphi/\hbar$.

6.1.2 Application to the Problem at Hand

Our goal is to invert the solution (6.1) to find $\varphi(t,r)$. Far enough from the source of these waves, the inverse Fourier transform becomes amenable to the method of stationary phase. The first step is to analyse the function:

$$\psi(\omega) = \frac{t}{r-r_{\rm ex}}\omega + \begin{cases} +\sqrt{\omega^2-\omega_\varphi^2} & \text{for } \omega < -\omega_\varphi \\ -\sqrt{\omega^2-\omega_\varphi^2} & \text{for } \omega > -\omega_\varphi \end{cases} \tag{6.3}$$

Solving $\psi'(\omega) = 0$ gives the solutions:

$$\Omega_\pm = \frac{\pm\omega_\varphi}{\sqrt{1-(r-r_{\rm ex})^2/t^2}} \tag{6.4}$$

Which gives a physical solution provided $r - r_{\rm ex} < t$, $\Omega_\pm$ being analogous to α in the section above. Observe that high frequency waves arrive first (as $t \downarrow (r-r_{\rm ex})$, $|\Omega_\pm| \to \infty$) while lower frequency waves arrive later. For this reason, the signal is described as an *inverse chirp*. Now we may use the method of stationary phase:

$$\begin{aligned} f(t,r) &= \frac{1}{2\pi}\sqrt{\frac{2\pi}{r-r_{\rm ex}}}\left(\frac{\tilde f(\Omega_+,r_{\rm ex})}{\sqrt{|\psi''(\Omega_+)|}}e^{i\psi(\Omega_+)(r-r_{\rm ex})+i\frac{\pi}{4}\text{sign}(\psi''(\Omega_+))} + \frac{\tilde f(\Omega_-,r_{\rm ex})}{\sqrt{|\psi''(\Omega_-)|}}e^{i\psi(\Omega_-)(r-r_{\rm ex})+i\frac{\pi}{4}\text{sign}(\psi''(\Omega_-))}\right) \\ &= \frac{1}{\sqrt{2\pi(r-r_{\rm ex})}}\frac{\tilde f(\Omega_+,r_{\rm ex})}{\sqrt{|\psi''(\Omega_+)|}} \times 2\mathcal{R}\big(e^{i\psi(\Omega_+)(r-r_{\rm ex})+i\frac{\pi}{4}\text{sign}(\psi''(\Omega_+))}\big) \qquad (\mathcal{R} \text{ denotes real part}) \\ &= \sqrt{\frac{2}{\pi(r-r_{\rm ex})}}\frac{\tilde f(\Omega_+,r_{\rm ex})}{\sqrt{|\psi''(\Omega_+)|}}\cos\big(-\psi(\Omega_+)(r-r_{\rm ex}) - \frac{\pi}{4}\text{sign}(\psi''(\Omega_+))\big) \end{aligned}$$

The factor of $1/(2\pi)$ in the first line is inherited from the definition of the inverse Fourier transform. In the second equality we used the fact that $\tilde f$ is even in its ω argument, as well as $\Omega_+ = -\Omega_-$ and that ψ (and its derivatives) are odd in the region $|\omega| > \omega_\varphi$. Evaluating the ψ, ψ'' terms and absorbing the sign dependence[10] of $\tilde f(\Omega_+, r_{\rm ex})$ into the cosine, we get $f(t,r) = A(t,r)\cos\phi(t,r)$, where $A(t,r)$ and $\phi(t,r)$ are given by:

$$\boxed{\begin{aligned} A(t,r) &= \sqrt{\frac{2}{\pi}}\frac{(\Omega^2-\omega_\varphi^2)^{3/4}}{\omega_\varphi(r-r_{\rm ex})^{1/2}}|\tilde f(\Omega,r_{\rm ex})| \qquad (6.5) \\ \phi(t,r) &= \sqrt{\Omega^2-\omega_\varphi^2}(r-r_{\rm ex}) - \Omega t - \frac{\pi}{4} + \text{Arg}\big[\tilde f(\Omega,r_{\rm ex})\big] \qquad (6.6) \end{aligned}}$$

Where $\Omega = \Omega_+$.

6.2 More Numerical Simulations

It is important to further numerically investigate the dynamics of core collapse in scalar-tensor gravity to check that dipole GW radiation is emitted at detectable levels from astronomical events that can be feasibly detected and observed. In this section we will outline the key results from several numerical studies investigating GW emission in ST gravity. The initial conditions and equations of state are in many cases the same or very similar to those discussed in section 5.2, and so no further discussion of them is presented here.

Long-Lived Inverse Chirp Signals From Core Collapse in Massive Scalar-Tensor Gravity [17]
This study simulates core collapse, finding that detectable levels of GW radiation remain present for relatively long times after the initial collapse event at distances 10 kpc from the source. Indeed, the inverse chirp is found to be nearly monochromatic over scales $\lesssim 1$ month, as we discussed in the previous section. Some results of this study are discussed in further detail in Figure 5.

[10] $\tilde f$ is real. To see this, $\overline{\tilde f(\omega,r)} = \int_{-\infty}^{\infty} e^{i\omega t} f(t,r)\, d\omega = \tilde f(-\omega,r) = \tilde f(\omega,r)$, where we used the fact $\tilde f$ is even in the ω argument, as previously discussed.

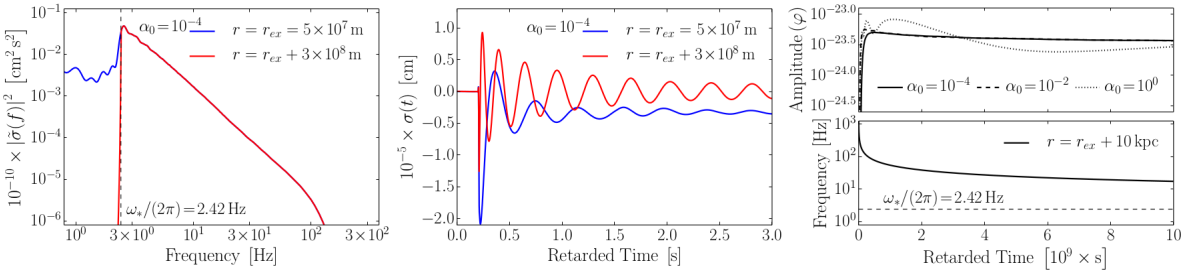

Figure 5: The results of the study [17], which show gravitational wave emission of the scalar field due to the core collapse of a $12M_\odot$ star. The simulation was run with $m_\varphi = 10^{-14}$eV, $\alpha_0 = 10^{-4}$ and $\beta_0 = -20$, with an extraction sphere 1 light second from the centre of the system. The left panel is the frequency-domain power spectrum of $\sigma = r\varphi$ seen at the extraction radius. Observe the sharp cut off at the frequency $\omega_\varphi/(2\pi)$, due to the exponential decay of lower frequencies (see equation (6.1) and surrounding text for an explanation of this). The centre panel gives the scalar field profiles of the two curves from the left panel plotted against time. In particular, note that the signal becomes increasingly oscillatory further out from the extraction sphere. The right hand figure shows how the amplitude and frequency (top and bottom resp.) of the scalar field φ vary as functions of time, extracted at a distance of 10 kpc from the source. In particular, notice that the signal is indeed inverse chirp as predicted, and that simulations run with different α_0 parameters (10^{-2} and 10^0) give similar amplitude profiles, demonstrating that the dependence of the amplitude of the scalar field on α_0 is only weak.

Numerical Simulations of Stellar Collapse in Scalar-Tensor Theories of Gravity [14]
As previously mentioned, this study investigates spherically symmetric core collapse for three different models of star (polytropic, WH12, WH40) with a polytropic equation of state. In addition to forming scalarized neutron stars (and black holes), significant dipole radiation is observed to be emitted. Further, such radiation is seen to be marginally detectable using current gravitational wave detectors, meaning we can start looking for evidence of scalar tensor gravity *now*.

Numerical Studies on Core Collapse Supernova in Self-interacting Massive Scalar-Tensor Gravity [19]
This study investigates the addition of a "self-interaction" term to the scalar potential, $V(\varphi) = 2m_\varphi^2\varphi^2 + 4\lambda\varphi^4$, with λ being the constant controlling the degree of self-interaction (the usual $A(\varphi) = \exp(\alpha_0\varphi + \beta_0\varphi^2/2)$ is used, with $\alpha_0 = 10^{-2}$ and $\beta_0 = -20$). It is found that inclusion of such a term significantly dampens the amount of detectable scalar radiation carried in gravitational waves. For instance, when λ is unity, the frequency-domain power spectrum is reduced to about 1% of its value in the non-interacting theory. This serves to demonstrate that although non-detection of scalar waves may constrain the massive theory, it cannot rule out the possibility of such a self interacting theory.

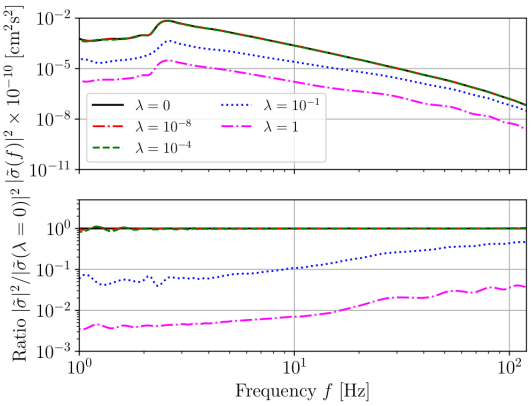

Figure 6: The effect of changing the parameter λ in a self interacting theory with scalar mass $m_\varphi = 10^{-14}$ eV, taken from [19]. The top pane shows the absolute magnitude of the frequency-domain power spectrum, while the bottom gives the ratio of the FDPS for different λ, compared to the non-interacting case $\lambda = 0$. In particular, it can be seen that larger λ values significantly suppress the spectral density when compared to the non-interacting theory (to about 1% when λ is unity), from which we infer that non-detection of a breathing mode in a GW cannot rule out self-interacting theories for which λ is sufficiently large.

6.3 The Smoking Gun

In GR, detectable gravitational waves appear as quadrupole (or even higher order) radiation. However, in ST gravity this is not the case - the scalar contribution to the wave first appears at the dipole order, and is referred to as a *breathing mode*. Detection of such a signal would therefore constitute so called *smoking gun* evidence of scalar-tensor gravity, whilst non-detection may allow us to further constrain the parameter space of the theory. We will outline several proposed methods of searching for these signals, which are possible with gravitational wave detectors available *now*, which are discussed in [17]:

- **Monochromatic searches**. The scalar signal described in equations (6.5) and (6.6) is nearly monochromatic on time scales of one month or less. Therefore, existing monochromatic all sky searches may be used to try and detect such a signal. In fact, greater success may be found by a *directed* search - when a nearby supernova is observed, we focus all attention to the GW radiation it has emitted. The non-detection of a GW attributed to a scalar field could constrain $\alpha_0 \lesssim 3\times10^{-4}$ for the massive theory, which is comparable to the Cassini bound obtained in the massless case [17]. Because the signal may remain present for so long, it may even be worth looking at nearby historical supernovae to see if any remnants of such a signal are still detectable as well.

- **Stochastic searches**. As we have seen, there is a well defined cut-off at $\omega_\varphi/(2\pi)$ in the frequency-domain power spectrum of the GW wave attributed to φ. Because the signal disperses, it is hard to detect this from far away sources. However, the signals from many distant overlapping GW sources will form a stochastic background signal with a characteristic spectral shape around the cut-off frequency, and analysis of such a signal could further constrain parameters in theory space.

- **Burst searches**. Because the GW radiation attributed to lighter scalar fields disperses less than those due to a heavier field, theories in which the scalar field is very light ($\mu \lesssim 10^{-20}$ eV) will not spread out significantly by the time they reach a GW interferometer on Earth. These "burst" like signals could be detected using similar methods to those already used for detecting supernovae in GR.

7 Conclusion

With the advent of gravitational wave interferometers, physicists are now able to observe the most energetic events known to exist in the universe, and thus probe the theory of general relativity in the strong field regime, where until recently it has been completely untested. Due to the recent success of quantum field theories, it is perhaps inevitable that the physical nature of gravity may deviate somewhat from that predicted by GR in this regime. While there are several theories one could choose for a modified theory of gravity, scalar-tensor gravity should be one of the favourites to test GR against because it predicts a completely new macroscopic phenomenon, the scalarized neutron star. Furthermore, the stellar core collapse that leads to the formation of such a star has been show by means of simulation to emit dipole gravitational wave radiation, another stark difference from GR, the observation of which would constitute "smoking gun evidence" that GR is not correct in the high energy limit. Furthermore, if we are lucky enough to have a relatively nearby supernova (~ 10 kpc [14, 17]) within our galaxy, such dipole modes may be detectable with the current generation of GW detectors. Even from a non-observation of such radiation we will be able to further constrain our theory, maturing our understanding of GR on the long and winding road to a complete unification of gravity and quantum field theory.

Due to the recent success in detecting black hole and neutron star mergers, future research could be devoted to analysing the expected waveforms emitted during this process. For instance, what might we expect to see when two scalarized neutron stars merge? It could be the case that even stronger emission dipole radiation is predicted, providing another scenario in which we may test GR against alternate theories of gravity. To this author's knowledge, only two studies have been done to date [9, 11], the first investigating neutron-neutron star mergers in massless ST gravity, and the second studying the merger of two black holes inside a "scalar field bubble" with a more unusual "inflationary inspired" potential. Both of these may be expanded upon by, for instance, investigating the effects of including a massive scalar field and extracting the waveforms of the gravitational waves emitted.

8 Appendix

8.1 Christoffel Symbols for Static Spherical Spacetime

These are easily derived by considering an appropriate action, or one can refer to [16] (although, in this reference, the symbols are derived the slow way from their definition). We've dropped the $*$ below corresponding to $g^*_{\mu\nu}$, but it should be understood to be there.

$$\begin{gathered}\Gamma^t_{tr} = \frac{1}{2}\nu'(r) \\ \Gamma^r_{tt} = \frac{1}{2}e^{\nu(r)}\left(1-\frac{2\mu}{r}\right)\nu'(r) \quad , \quad \Gamma^r_{rr} = \frac{\mu' r - \mu}{r(r-2\mu)} \quad , \quad \Gamma^r_{\theta\theta} = 2\mu - r \quad , \quad \Gamma^r_{\phi\phi} = \sin^2\theta(2\mu - r) \\ \Gamma^\theta_{r\theta} = \frac{1}{r} \quad , \quad \Gamma^\theta_{\phi\phi} = -\sin\theta\cos\theta \\ \Gamma^\phi_{r\phi} = \frac{1}{r} \quad , \quad \Gamma^\phi_{\theta\theta} = \cot\theta\end{gathered} \tag{8.1}$$

(With all other symbols vanishing).

References

[1] K. J. Nordtvedt, *Astrophys. J. 161: 1059-67(Sep 1970).* **1970**, *161*, DOI 10.1086/150607.

[2] T. Damour, G. Esposito-Farèse, *Phys. Rev. Lett.* **1993**, *70*, 2220–2223.

[3] J. D. Bekenstein, Black hole hair: twenty–five years after, **1996**.

[4] T. Damour, G. Esposito-Farse, *Physical Review D* **1996**, *54*, 14741491.

[5] S. M. Carroll, Lecture Notes on General Relativity, **1997**.

[6] B. Bertotti, L. Iess, P. Tortora, *Nature* **2003**, *425*, 374–376.

[7] S WOOSLEY, A HEGER, *Physics Reports* **2007**, *442*, 269283.

[8] P. C. C. Freire, N. Wex, G. Esposito-Farse, J. P. W. Verbiest, M. Bailes, B. A. Jacoby, M. Kramer, I. H. Stairs, J. Antoniadis, G. H. Janssen, *Monthly Notices of the Royal Astronomical Society* **2012**, *423*, 3328–3343.

[9] J. Healy, T. Bode, R. Haas, E. Pazos, P. Laguna, D. M. Shoemaker, N. Yunes, *Classical and Quantum Gravity* **2012**, *29*, 232002.

[10] J. Antoniadis, P. C. C. Freire, N. Wex, T. M. Tauris, R. S. Lynch, M. H. van Kerkwijk, M. Kramer, C. Bassa, V. S. Dhillon, T. Driebe, J. W. T. Hessels, V. M. Kaspi, V. I. Kondratiev, N. Langer, T. R. Marsh, M. A. McLaughlin, T. T. Pennucci, S. M. Ransom, I. H. Stairs, J. van Leeuwen, J. P. W. Verbiest, D. G. Whelan, *Science* **2013**, *340*, DOI 10.1126/science.1233232.

[11] E. Barausse, C. Palenzuela, M. Ponce, L. Lehner, *Physical Review D* **2013**, *87*, DOI 10.1103/physrevd.87.081506.

[12] C. M. Bender, *Advanced mathematical methods for scientists and engineers. 1, Asymptotic methods and perturbation theory / Carl M. Bender, Steven A. Orszag.* Springer, Delhi, **2013**.

[13] C. A. R. Herdeiro, E. Radu, Asymptotically flat black holes with scalar hair: a review, **2015**.

[14] D. Gerosa, U. Sperhake, C. D. Ott, *Classical and Quantum Gravity* **2016**, *33*, 135002.

[15] F. M. Ramazanolu, F. Pretorius, *Physical Review D* **2016**, *93*, DOI 10.1103/physrevd.93.064005.

[16] B. Kumar, Derivation of TOV equations, **2017**.

[17] U. Sperhake, C. J. Moore, R. Rosca, M. Agathos, D. Gerosa, C. D. Ott, *Physical Review Letters* **2017**, *119*, DOI 10.1103/physrevlett.119.201103.

[18] C. M. Will, *Theory and Experiment in Gravitational Physics*, 2nd ed., Cambridge University Press, **2018**.

[19] P. C.-K. Cheong, T. G. F. Li, *Physical Review D* **2019**, *100*, DOI 10.1103/physrevd.100.024027.